[Frontiers in Bioscience 10, 268--274, January 1, 2005]

SURFACE PLASMON RESONANCE SPECTROSCOPY AND QUARTZ CRYSTAL MICROBALANCE STUDY OF MUTS BINDING WITH SINGLE THYMINE-GUANINE MISMATCHED DNA

Xiaodi Su,[1] Ying-Ju Wu,[1] Rudolf Robelek [1] and Wolfgang Knoll [1, 2]

[1] Institute of Materials Research and Engineering, 3 Research Link, Singapore 117602, [2] Max-Planck-Institut für Polymerforschung, Ackermannweg 10, 55128 Mainz, Germany

TABLE OF CONTENTS

1. ABSTRACT

MutS is a DNA mismatch binding protein that recognizes heteroduplex DNA containing mispaired or unpaired bases. In this study, we employ a quartz crystal microbalance (QCM) and a surface plasmon resonance (SPR) device for the study of MutS binding with DNA containing a single Thymine-Guanine (T-G) mismatch at different sites. Multi-step surface binding reactions are involved in the study, including probe DNA immobilization on the sensor surface through biotin-streptavidin-biotin bridge chemistry, target DNA hybridization to form T-G heteroduplexes, and MutS recognition of the mutation sites. The QCM frequency (Δf) and motional resistance (ΔR, an impedance parameter reflective of QCM damping), as well as the SPR angle shift ($\Delta\theta$) are recorded for the binding reactions. The combined SPR and QCM data collection and analysis allow for an assessment of not only the amount of bound biopolymer but provide also information on also the structural properties of the streptavidin, DNA and MutS/DNA complexes. The affinity of the MutS/T-G heteroduplex assembly is determined by both the QCM and SPR methods through titration of the surface bound DNA with increasing MutS concentration. It is found that if the T-G mismatch is in the center of the DNA fragment, the MutS/DNA complex is more stable than if the mismatch is located near the end of the fragment.

2. INTRODUCTION

MutS is a DNA mismatch binding protein that binds to DNA containing mismatched base pairs and unpaired bases but not equally well to fully matched DNA. The mismatch-binding activity of the MutS protein has been exploited for the detection of DNA mutations in several formats, including a nitrocellulose membrane based chemiluminescence assay (1), a MutS exonuclease protection assay (2), by atomic force microscopy imaging of MutS/DNA complexes (3, 4), and by DNA-chip/protein-chip based fluorescent assays (5, 6).

Biosensors are analytical devices that incorporate biological elements with physicochemical transducers or transducing systems. Being able to convert biological events into measurable signals of different physical formats, biosensors have proven to be versatile in biomedical research and biological analysis. Earlier employments of biosensors for the study of MutS/DNA interactions were reported by Babic et al (7) and Gotoh et al (8), who applied surface plasmon resonance (SPR) spectroscopy to monitor MutS binding with surface-bound DNA in a label free format. The follow up applications of the SPR technique in the research of similar subjects include studies of ATP modulated MutS/DNA binding (9), MutS affinity with heteroduplexes containing different mismatches (5), and DNA binding with synthesized mismatch binding ligands (10, 11).

Quartz crystal microbalance (QCM), similar to SPR spectroscopy, is another label-free technique, capable of on-line monitoring of biomolecular binding reactions. In a recent study, we demonstrated the first incorporation of MutS based mismatch recognition with QCM measurements for small gene alternation detection (12). Through the measurements of the selective MutS bindings, discriminations between fully matched DNA and single base mismatched DNA (and DNA containing 1-4 unpaired loops) were achieved.

Among many biosensor formats, SPR and QCM become known as complementary techniques suitable for *in-situ* monitoring of interfacial processes. One of the current trends in SPR and QCM research is to use a combination of SPR and QCM data collection and analysis to obtain complementary understandings of a particular binding event (13-16). This becomes possible as QCM and SPR are based on different physical principles; each being sensitive to different properties of the materials studied. SPR spectroscopy, for example, is an optical technique that detects changes in the refractive index of thin films assembled on a noble-metal surface. The SPR angle shifts are related to the thickness of the assembled films. On the other hand, QCM measures acoustic thickness of thin films mechanically coupled to a metal electrode on quartz disks. QCM oscillation frequency and quality are related to the mass loading and the viscoelastic properties of the adsorbed materials. Using the combined QCM and SPR data one can assess not only the binding amounts but also the structural properties of molecules studied (15, 16).

Table 1. Nucleotide sequences of the probe DNA and target DNA used in this study

Names	**Nucleotide Sequence**
Probe DNA	Biotin- 5'- GCA CCT GAC TCC TG***T*** GGA GAA GTC ***T***GC CGT-3'
T·A target	3'-CGT GGA CTG AGG AC***A*** CCT CTT CAG ACG GCA-5'
Probe DNA	Biotin- 5'- GCA CCT GAC TCC TG***T*** GGA GAA GTC ***T***GC CGT-3'
T-G target (centre)	3'-CGT GGA CTG AGG AC***G*** CCT CTT CAG ACG GCA-5'
Probe DNA	Biotin- 5'- GCA CCT GAC TCC TG***T*** GGA GAA GTC ***T***GC CGT-3'
T-G target (end)	3'-CGT GGA CTG AGG ACA CCT CTT CAG ***G***CG GCA-5'

In the current study, we apply in parallel a SPR instrument and a QCM device for the study of MutS binding with heteroduplex DNA containing single T-G mismatches. A 30 mer single-stranded probe DNA is immobilized on the sensor surfaces through biotin-streptavidin-biotin bridge chemistry. Target DNAs containing a single base substitution (A→G) in the centre or near the end of the sequence are hybridized with the probe DNA to form T-G heteroduplexes with the mismatch located at different sites. The MutS protein is then applied to bind to the mismatch sites. The affinities of the MutS/T-G heterodulpexes are determined by both the QCM and SPR methods, through the titration of the surface bound DNA with increasing MutS concentrations. As a control sample, fully complementary target DNA is also hybridized with the probe DNA to form T·A homoduplex for testing the sequence independent MutS binding. Our focus is set on T-G mismatch type because of its enormous high importance especially in the field of cancer research and diagnostics. This becomes very clear when one looks at the IARC database, which contains over 18,000 entries of cancer related mutations of the human p53 gene. An analysis of the entries shows that almost a quarter of the mutations in this gene are cytosine to thymine transitions which cause T-G mismatch situations (17, 18).

Other than in our previous work (12), where a protocol for the discrimination between MutS/T-G and MutS/T·A through QCM frequency measurements was developed, the QCM in this study is operated using a network analyzer, by which oscillation frequency (f) and motional resistance (R) are recorded simultaneously. The latter is an impedance parameter derived form a QCM equivalent circuit, being reflective of the damping of the oscillation (19). The simultaneously measured Δf and ΔR allow an assessment of the viscoelastic property of the protein and DNA layers. In combination with the SPR angle shifts ($\Delta\theta$) from the parallel SPR measurements, we are able to extend our understanding of the protein and DNA bindings from affinity and kinetics to molecular conformations.

3. MATERIALS AND METHODS

3.1. Materials

Thermostable MutS protein derived from the thermophilic bacterium *Thermus aquaticus* was purchased from Epicentre Technologies (Madison, WI, US). This protein (20 mM) is supplied in a 50 % glycerol solution containing 50 mM tris-HCl (pH 7.5), 100 mM NaCl, 1 mM dithiothreitol, 0.1 mM EDTA and 0.1% Triton X-100. Streptavidin (SA) was purchased from Sigma-Aldrich (St. Louis, MO). Biotin- and PEG- terminated alkanethiols, used for the preparation of the gold surfaces, were synthesized in our laboratory at the Max-Planck-Institute for Polymer Research (Mainz).

The MutS/DNA binding buffer was a 50 mM tris-HCl (pH 7.5) solution containing 100 mM NaCl, 1mM dithiothreitol, 0.1 mM EDTA, and 5 mM $MgCl_2$. HEPES buffer (50 mM HEPES, 25 mM NaOH, 75 mM NaCl) was used for DNA immobilization and target DNA hybridization. PBS buffer was used for streptavidin immobilization.

Highly purified salt free (HPSF) oligonucleotides were obtained from MWG (Germany). The sequences of the oligonucleotides are summarized below. The probe DNA is provided with a biotin label at the 5' end. The T·A target is fully complementary to the probe DNA. The T-G target DNAs contains a single base substitution (A→G) either at the center ['T-G target (center)'] or near the 5' end ['T-G target, (end)']. By probe / target DNA hybridization, T-G heteroduplexes can be formed so that the mismatch sites are either located in the centre or near the end of the DNA duplex (Table 1).

3.2. QCM measurement

AT-cut, 10 MHz quartz crystals with polished gold electrodes (International Crystal Manufacture Co. Inc., Oklahoma City, OK, USA) were used as reaction carriers. These crystals provide a mass sensitivity of 1 Hz = 4.4 ng/cm^2 for rigid and ultra thin coatings. For in-situ oscillation measurements in liquid, the crystals were fixed into two Plexiglas blocks with Neoprene *O*-ring seals. The upper face of the crystals was exposed to 100 μL of the sample solutions. The setup was connected to a S&A 250B Network Analyzer (Saunders & Associates, Inc. USA), with which oscillation frequency and motional resistance responses were recorded simultaneously. The measurements were carried out at room temperature. The response draft of frequency and motional resistance due to temperature fluctuations, pressure changes and mechanical disturbances etc were 2 Hz and 0.1 Ω, respectively.

3.3. SPR measurement

The SPR measurements were conducted using a double channel, AUTOLAB ESPR (Eco Chemie, The Netherlands). The configuration of this equipment is described elsewhere (20). Briefly, p-polarized laser light

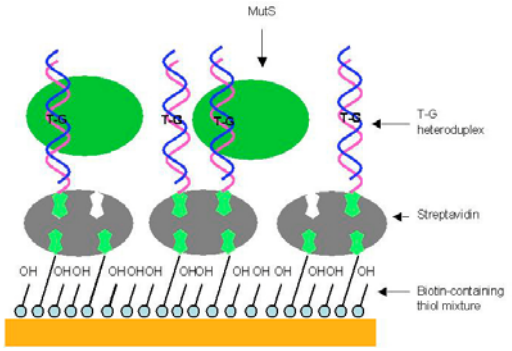

Figure 1. Schematic illustration of the surface architecture used for the assay, including SA immobilization on biotin-containing thiols treated surface, biotin-DNA attachment through biotin-SA binding, target DNA hybridization, and finally MutS protein recognition of the mismatch.

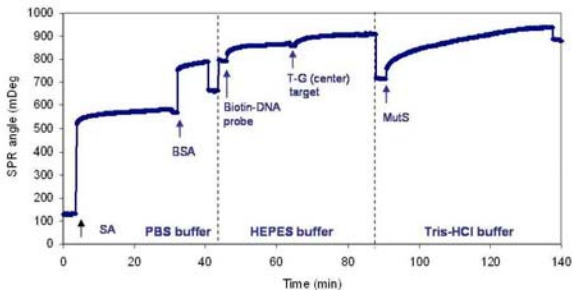

Figure 2. SPR measurement of the binding reactions shown in scheme 1. SA immobilization and BSA blocking is conducted in PBS buffer. Prior to the probe DNA immobilization and target (T-G center) hybridization the surface is calibrated in HEPES buffer. The MutS binding to the T-G heteroduplex is in tris-HCl buffer.

(λ=670 nm) is directed via a hemicylindrical lens to the bottom side of the sensor disk and the reflected light is detected by a photodiode.The angle of incidence is varied using a vibrating mirror with a frequency of 44 Hz. In each cycle, SPR curves were scanned on the forward and backward movement of the mirror. In an adjustable interval time, the minimums in reflectance are determined and averaged. Binding curves are obtained by processing this minimum in reflectance in real-time. The instrument is equipped with a cuvette. The gold sensor disks (diameter 17 mm) mounted on the lens (through index-matching oil) form the base of the cuvette. An autosampler (Eco Chemie, The Netherlands) is used to inject or remove the tested solutions. The measurements were carried out at room temperature. The noise of the SPR angle is 5 mDegrees.

4. RESULTS AND DISCUSSION

4.1. SPR and QCM measurements of the binding reactions

Figure 1 is a schematic illustration of the multi-layer surface architecture used in this study. The gold electrode is first treated with a binary mixture of biotin- and OH-terminated alkanethiols as described in the previous study (12). The formation of a biotin-containing self-assembled monolayer (SAM) on the surface allows for the attachment of a streptavidin (SA) layer through biotin-SA linkages. Figure 2 shows the SPR angle shift ($\Delta\theta$) measured for the reactions schematized in Figure 1, starting from the SA immobilization on the binary SAM treated surface in PBS buffer. After the SA immobilization, BSA (5 % in PBS) was applied for blocking the unoccupied surface in order to minimize the possible nonspecific binding of the DNA and MutS in the following steps. The application of the probe DNA (1 μM) followed by the target DNA [T-G target (centre), 1 μM] in HEPES buffer results in sequential $\Delta\theta$ increases, indicative of the formation of a surface bound DNA duplex. After calibrating the surface using the MutS binding buffer blank (a tris-HCl buffer containing the same amount of glycerol and triton X-100 as the MutS protein solution of the practical concentration), MutS protein (100 nM) is applied. The binding of the protein to the T-G heteroduplex DNA is detected as a steady $\Delta\theta$ increase in the association phase followed by a certain degree of $\Delta\theta$ decrease in the dissociation phase. Using the AUTOLAB SPR sensitivity of 120 mdegree = 100 ng/cm^2, the measured $\Delta\theta$ for each reaction step can be converted to mass uptake (Δm_{SPR}) in terms of ng/cm^2 (see insets in Figure 3 and Table 2 below).

The same binding reactions were also detected using the QCM with impedance analysis. The accumulation of the protein and DNA molecules on the QCM surface are detected as a stepwise frequency decrease (Δf) accompanied by a motional resistance increase (ΔR), with different $\Delta R/\Delta f$ ratios, depending on the viscoelasticity of the film (16). Figure 3 shows the QCM responses (Δf and ΔR) for the key reaction steps, namely SA immobilization (Figure 3A), probe DNA and target DNA assembly (Figure 3B), and MutS binding (Figure 3C). The QCM mass uptakes (Δm_{QCM}), converted from the measured frequency decreases using the Sauerbrey mass sensitivity of 1 Hz = 4.42 ng/cm^2 for the 10 MHz QCM, and the SPR mass uptakes of the corresponding reaction steps (Δm_{SPR}) are included in the insets in the Figures. The differences between the Δm_{QCM} and Δm_{SPR} are found to be relative of the viscoelastic property of the adsorbed macromolecules, which can also be revealed by the ΔR values (see below).

For the SA film formation (Figure 3A), the steady frequency decrease is accompanied with a barely detectable ΔR increase. It has been shown in previous studies that the SA molecules assembled on a biotin-containing surface are in a highly ordered 2-D arrangement with two of the biotin binding sites being occupied and the other ones facing towards the solution (15, 21). The barely detectable ΔR increase measured here by the QCM indicates that the well-ordered SA film exhibits a rigid structure. The molecular film can fully couple with the oscillation with negligible energy dissipation. For such a stiff film, the measured Δf contains mostly the mass effect but no viscoelasticity contribution (19). Thus the measured Δf value can be used to calculate the mass loading. This explains why the QCM mass for the SA film is rather close to the SPR mass (differing in a factor of 1.2). The latter is believed to be better reflective of the molecular mass of the protein film (16).

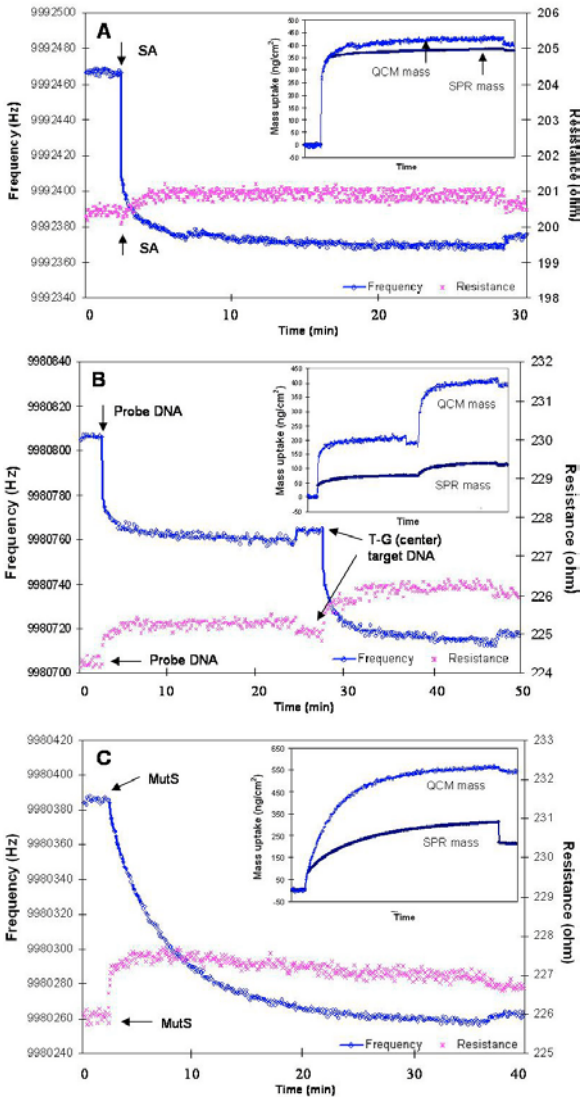

Figure 3. QCM response (f and R) to (A) SA immobilization on the biotin-containing surface, (B) probe DNA assembly and T-G (center) target DNA hybridization, and (C) MutS recognition of the heteroduplex DNA. The QCM mass uptakes, converted from the measured Δf and the Sauebrey sensitivity (1 Hz = 4.4 ng/cm^2) of the 10 MHz QCM, are included in the insets. For comparison the SPR mass uptake for each corresponding reaction are also presented.

For the DNA assembly (Figure 3B), the molecular accumulation on sensor surfaces (Δf decreases) results in a remarkable ΔR increase, indicating the formation of highly dissipative molecular layers (16, 19). It is generally agreed that for DNA molecules, great amounts of solvent molecules are entrapped via direct hydration or viscous drag (15). The DNA layers are essentially sensed by the QCM as viscoelastic brush composed of the macromolecules and the coupled solvent. For the specific DNA system involved in this study, we do observed a 3-4 times greater QCM mass over the SPR mass (dry mass or molar mass). The simultaneously measured ΔR increases are the essential measures of the viscoelastic properties of the DNA layers.

For the MutS binding with a T-G heteroduplex (Figure 3C), the ΔR response shows a non-monotonous trend throughout the MutS/T-G heteroduplex complex formation, *i.e.* an initial rise of R is followed by a slow R decrease during the completion of the complex formation. This indicates the formation of an initial dissipative protein film followed by the formation of a more rigid structure. The formation of the initial dissipative protein film may correspond to the clamping process of the MutS protein dimer to the DNA and the scanning process to locate the mismatch site (22). The second phase ΔR response (ΔR decrease) may be attributed to the conformational change of the MutS protein, when it takes up a more compact structure via strong hydrogen bonds between the thymine/guanine bases and its mismatch binding domain and its wedging into the kinked DNA backbone once the mismatch recognition is accomplished (23, 24). Thus the ΔR pattern measured with the QCM can be used as a 'fingerprint' for the different MutS/DNA complex formation stages. For the dissipative MutS layer, the QCM mass uptake measured 5 min after the dissociation phase is ~2 times of Δm_{SPR} at the same dissociation stage.

Table 2 summarizes the QCM data (Δf, ΔR, $\Delta R/\Delta f$, and Δm_{QCM} for each step at saturation) and the corresponding SPR results (Δm_{SPR}). The ratio of $\Delta R/\Delta f$ (induced energy loss per coupled unit mass) is reflective of the viscoelasticity or flexibility of the film. As a general trend, the more dissipative the film (represented by the higher $\Delta R/\Delta f$ value) the bigger is the difference between Δm_{QCM} and Δm_{SPR}. Thus for any macromolecular films, the combined QCM and SPR data would provide an assessment of the film structure or molecular orientation as different molecular structure would lead to different viscoelasticity.

4.2. Discrimination between T-G heteroduplex and T·A homoduplex

Figure 4 shows the SPR measurements of the hybridization of the T·A target and T-G (center) target, respectively, with the surface bound probe DNA, followed by the MutS binding with the resulting T·A homoduplex and T-G heteroduplex. The target hybridization shows no detectable difference in the saturated amount and kinetics as the single base substitution in the 30 pb DNA does not introduce sufficient affinity decline. However, the subsequent MutS application results in a clear discrimination between the fully matched and mismatched DNA. The greater $\Delta\theta$ increase and slight dissociation for the T-G heteroduplex is due to the specific mismatch recognition and the weaker nonspecific binding and drastic dissociation from the T·A homoduplex is due to a sequence independent contact (23).

A similar discrimination is also obtained from the QCM measurements (Figure 5). In Figure 5 we also show the MutS binding to a T-G heteroduplex with the mutation site located near the far end of the surface, formed through

Table 2. Summary of QCM and SPR data

Steps	Δf (Hz)	ΔR (Ω)	$\Delta R/\Delta f$ (mΩ/Hz)	Δm_{QCM} (ng/cm^2)	Δm_{SPR} (ng/cm^2)	$\Delta m_{QCM} / \Delta m_{SPR}$
SA	98.5±5.2	--- [1]	---	435.4±23.0	373.5±17.2	1.2
Probe DNA	46.2±4.1	0.91±0.08	19.7	204.2±18.1	74.7±30.2	2.8
Target DNA (T-G center)	49.5±4.6	1.12±0.10	22.6	218.8±20.3	49.8±25.3	4.4
MutS/T-G duplex [2]	105±7.6	0.65±0.08	4.5	464±33.6	232.4±24.1	2.0

[1] Barely detectable *R* increase; [2] Values from 5 min after disassociation

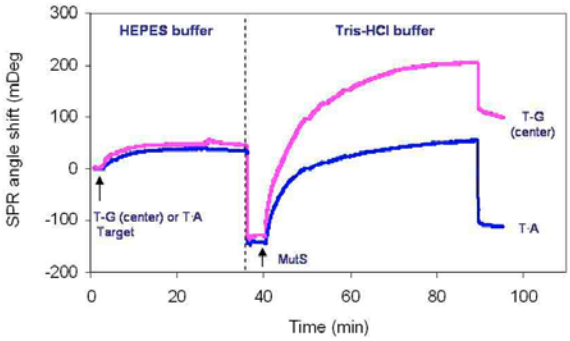

Figure 4. SPR measurements of the T·A and T-G (centre) target hybridization and the subsequent MutS binding with the formed T·A homoduplex and T-G heteroduplex DNA. Prior to the MutS application, the surface is calibrated with the tris-HCl buffer.

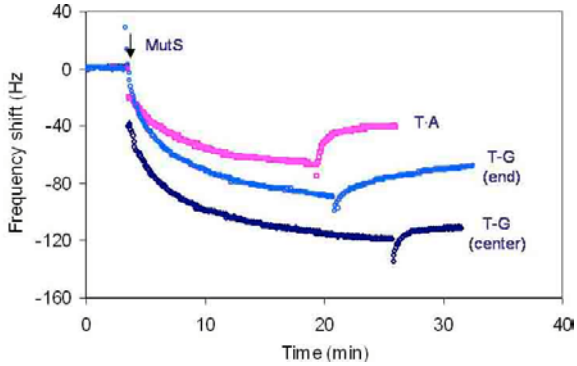

Figure 5. QCM measurements of the MutS bindings with T·A homoduplex, T-G (centre) heteroduplex, and T-G (end) heteroduplex DNA.

hybridization of the T-G (end) target with the probe DNA. The observed binding signal of a saturated amount of the DNA/MutS binding complex is lower in intensity and faster in dissociation kinetics than that of the T-G mismatch at the center. We attribute the difference in the binding amount and kinetic to the mechanism of the mismatch recognition and complexation by the MutS protein. For a stable complexation of the T-G mismatch, two processes are important: Firstly, MutS has to kink DNA at the mismatch site to allow for the wedging of the stabilizing bases into the DNA backbone. Secondly, the complete mismatch/MutS complex has to be stabilized by extensive interactions of four MutS domains with the DNA. These interactions surround up to 8 base pairs flanking the recognized mismatch location (24). In case of the T-G (end) target hybridizing with the probe DNA, the remaining 5 bases at the double strand's sequence end are not enough for the stabilization of the binding complex, while a mismatch located in the center of the 30 bp DNA offers enough flanking bases to allow for all necessary interactions.

4.3. Estimation of affinities of MutS/T-G heteroduplexes

To assess the binding affinity of the MutS/T-G heteroduplexes (centre or end), the dissociation constants (K_d) were estimated by titration of surface bound DNA with increasing concentrations of MutS. Both the QCM and SPR methods were used for the measurements. Figure 6 shows the titration curves measured by the QCM. The MutS protein at serial dilutions of 1/800, 1/400, 1/200, 1/100, 1/50 (corresponding to concentrations of 25, 50, 100, 200, 400 nM) was applied sequentially on the QCM that carries the T-G (end) heteroduplex DNA, upon equilibration for ~20 min at each individual concentration. Since the MutS protein is supplied in tris-HCl buffer containing 50 % glycerol and 0.1 % Triton X-100, the MutS signal at different MutS concentrations contains certain density/viscosity contributions depending on the dilution ratio. Therefore, a blank titration experiment (exposing the SA/BSA treated QCM carrying no DNA to the same series of protein solutions) was conducted. The blank frequency response was recorded as shown in Figure 6. By subtracting the frequency shifts of the blank titration (Δf_{blank}) from the equilibrium Δf_{MutS} of each corresponding MutS concentration, net $\Delta f_{MutS-net}$ caused by the MutS binding were obtained. The same titration experiment was also conducted for the T-G (center) heteroduplex DNA (curve not shown). Plotting the net $\Delta f_{MutS-net}$ as a function of MutS concentrations gives the known Langmuir adsorption isotherm (Figure 7). The full curves (T-G center and T-G end) are fitted to a Langmuir isotherm using non-linear least squares analysis to yield K_d values of 72.1 ± 2.3 nM and 101.7 ±3 .7 nM for the T-G (center) and T-G (end) duplex DNA, respectively.

Equivalent titration reactions were also measured using the double-channeled SPR instrument. Figure 8 shows the SPR MutS titration curves for the T-G (center) and T-G (end) DNA conducted simultaneously in one experiment from two channels, each carries a different T-G heteroduplex. To eliminate the refractive index effect caused by the buffer contents (mainly the glycerol and the triton X-100), a blank titration was detected by exposing the SA/BSA treated surface to the MutS protein solutions of increased concentrations. The obtained blank angle shifts are subtracted from the $\Delta\theta_{MutS}$. The plots of the net $\Delta\theta_{MutS-net}$ against the MutS concentrations are fitted using the same non-linear regression (fitting curves not shown). The K_d

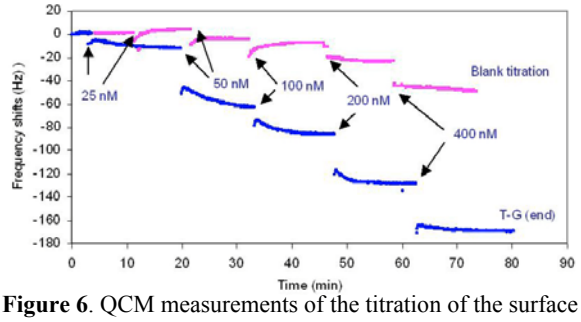

Figure 6. QCM measurements of the titration of the surface bound T-G (end) heteroduplex DNA using MutS at increased concentrations of 25, 50, 100, 200, and 400 nM and the titration of a SA/BSA treated surface carrying no DNA using the same series of MutS solutions. The arrows indicate the time when MutS solutions are applied.

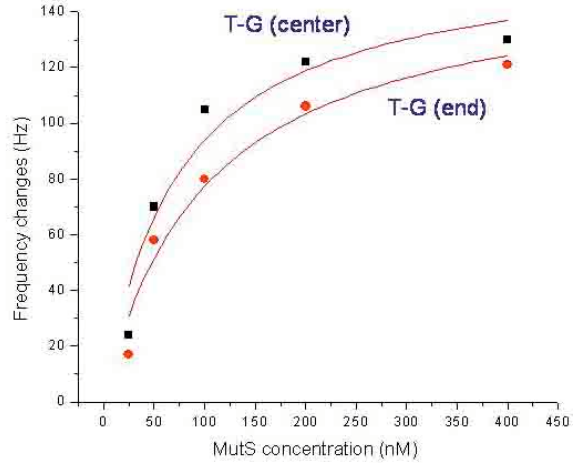

Figure 7. Plots of QCM $\Delta f_{\text{MutS-net}}$ vs MutS concentrations (dots) and the non-linear Langmuir curve fitting (lines).

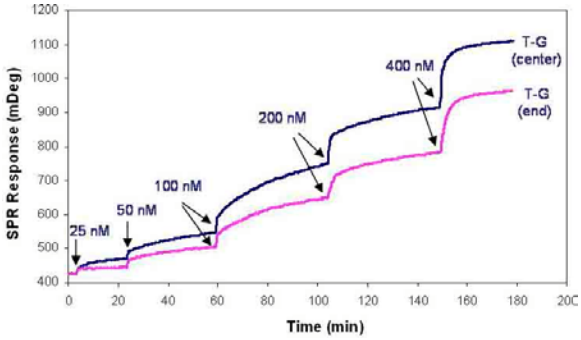

Figure 8. SPR measurements of the titration of the surface bound T-G (end) heteroduplex DNA and T-G (center) heteroduplex DNA using MutS at increased concentrations of 25, 50, 100, 200, and 400 nM. The arrows indicate the time when MutS solutions are applied.

values obtained are 134.5 ± 4.9 nM and 233.1 ± 3.9 nM, respectively.

In a previous study (9) K_d for a MutS/T-G heteroduplex of 41 bp DNA (mismatch at center) was reported as 21 nM and 30 nM at the salt concentrations of the binding buffer of 50 mM KCl and 150 mM KCl, respectively. Considering the differences in the salt concentration used in this study (100 mM NaCl) and the effects of different flanking sequences in the 30 bp DNA of this study and the 41 bp DNA in the literature, the K_d values obtained in this study are fairly reliable. As for the measured affinity decline when the T-G mismatch is moved to the end [T-G (end)], although there are no systematic studies of mismatch position dependence of MutS/T-G affinity that we can refer to, the previously reported MutS/T-G crystal structure would be a very good support of our observation (23, 24). According to the MutS/T-G crystal structure, the formation of a stable MutS/T-G complex depends on a sufficient number of flanking bases (up to 8) around the mismatch area. The smaller number of franking bases (5 bases) on one side of the T-G (end) target in this study would be responsible for the weaker binding.

5. CONCLUSION

We have demonstrated that QCM and SPR are complementary techniques for the study of biomolecular binding reactions. For protein/DNA binding assays, the combination of QCM and SPR data collection and analysis provides furthermore insights into the architecture of the single surface layers and a 'fingerprint' of the MutS/DNA binding mechanism, reflecting the different interaction phases. QCM and SPR are also proven to be powerful tools for study of binding affinities without the involvement of labeled materials. For the MutS/T-G heteroduplex for example, different binding affinities are obtained if the mismatch sites are located at different positions. Our further work will concentrate on the evaluation of the effect of the flanking sequence on the affinity of the MutS/T-G complex.

6. REFERENCES

1. Wagner R. E. & M. Radman: Mutation detection using immobilized mismatch binding protein (MutS). *Nucleic Acids Res* 23, 3944-3948 (1995)
2. Ellis L. A., G. R. Taylor, R. Banks & S. Baumberg: Muts binding protects heteroduplex DNA from exonuclease digestion in-vitro - A simple method for detecting mutations. *Nucleic Acids Res* 22, 2710-2711 (1994)
3. Zhang Y., Y. Lu, J. Hu, X. Kong, B. Li, G. Zhao & M. Li: Direct detection of mutation sities on stretched DNA by atomic force microscopy. *Sur Interface Anal* 33, 122-125 (2002)
4. Bin H. & H. Yokota: MutS-mediated detection of DNA mismatches using atomic force microscopy. *Anal Chem* 72, 3138-3141 (2000)
5. Behrensdorf H. A., M. Pignot, N. Windhab & A. Kappel: Rapid parallel mutation scanning of gene fragments using a microelectronic protein-DNA chip format. *Nucleic Acids Res* 30, e64 (2002)
6. Bi L. J., Y. F. Zhou, X. E. Zhang, J. Y. Deng, Z. P. Zhang, B. Xie & C. G. Zhang: A MutS-based protein chip for detection of DNA mutations. *Anal Chem* 75, 4113-4119 (2003)
7. Gotoh M., M. Hasebe, T. Ohira, Y. Hasegawa, Y. Shinohara, J. Sota, H. Nakao & M. Tosu: Rapid method for

detection of point mutations using mismatch binding protein (MutS) and an optical biosensor. *Genetic Analysis*: Biomolecular Engineering 14, 47-50 (1997)
8. Babic I., S. E. Andrew & F. R. Jirik: MutS interaction with mismatch and alkylated base containing DNA molecules detected by optical biosensor. *Mutation Res* 372, 87-96 (1997)
9. Blackwell L. J., K. P. Bjornson, D. J. Allen & P. Modrich: Distinct MutS DNA-binding modes that are differentially modulated by ATP binding and hydrolysis. *J Biol Chem* 276, 34339-34347 (2001)
10. Kobori A., S. Horie, H. Suda, I. Saito & K. Nakatan: The SPR sensor detecting Cytosine-Cytosine mismatches. *J Am Chem Soc* 126, 557-562 (2004)
11. Hagihara S., H. Kumasawa, Y. Goto, G. Hayashi, A. Kobori, I. Saito & K. Nakatani: Detection of Guanine-Adenine mismatches by surface plasmon resonance sensor carrying naphthyridine-azaquinolone hybrid on the surface. *Nucleic Acids Res* 32, 278-286 (2004)
12. Su X. D., R. Robelek, Y. J. Wu, G. Y. Wang & W. Knoll: Detection of point mutation and insertion mutations in DNA using quartz crystal microbalance and MutS, a mutation binding protein. *Anal Chem* 76, 489-494 (2004)
13. Su X. D. & J. Zhang: Comparison of surface plasmon resonance spectroscopy and quartz crystal microbalance for human IgE quantification. *Sens Actuators B* 100, 311-316 (2004)
14. Baily L. E., D. Kambhampati, K. K. Kanazawa, W. Knoll & C. W. Frank: Using surface plasmon resonance and the quartz crystal microbalance to monitor in situ the interfacial behavior of thin organic films, *Langmuir* 18, 479-484 (2002)
15. Larsson C., M. Rodahl & F. Höök: Characterization of DNA immobilization and subsequent hybridization on a 2D arrangement of streptavidin on a biotin-modified lipid bilayer supported on SiO2. *Anal Chem* 75, 5080-5087 (2004)
16. Höök F., B. Kasemo, T. Mylander C. Fant, K. Sott & H. Elwing: Variations in coupled water, viscoelastic properties, and film thickness of a Mefp-1 protein film furing adsorption and cross-linking: A quartz crystal microbalance with dissipation monitoring, ellipsometry, and surface plasmon resonance study. *Anal Chem* 73, 5796-5804 (2001)
17. Hernandez-Boussard T., P. Rodriguez-Tome, R. Montesano & P. Hainaut. IARC p53 mutation database: a relational database to compile and analyze p53 mutations in human tumors and cell lines (International Agency for Research on Cancer), *Hum Mutat* 14, 1–8 (1999)
18. Hollstein M., B. Shomer, M. Greenblatt, T. Soussi, E. Hovig, R. Montesano & C.C. Harris. Somatic point mutations in the p53 gene of human tumors and cell lines: updated compilation, *Nucleic Acids Res* 24, 141–146 (1996)
19. Calvo E. J., R. Danilowicz & R.J. Etchenique: Measurement of viscoelastic changes at electrodes modified with redox hydrogels with a quartz-crystal device. *J Chem Soc-Faraday Trans* 91, 4083-4091 (1995)
20. Wink T., S. J. Van Zuilen, A. Bult & P. van Bennekom: Interaction between plasmid DNA and cationic polymers studied by surface plasmon resonance spectroscopy. *Anal Chem* 70, 827-832 (1998)
21. Knoll W., M. Zizlsperger, T. Liebermann, S. Arnold, A. Badia, M. Liley, D. Piscevic, F. J. Schmitt & J. Spinke: Streptavidin arrays as supramolecular architectures in surface-plasmon optical sensor formats. *Colloids and Surface A: Physchem Eng Aspects* 161, 115-137 (2000)
22. Sixma T. K.: DNA mismatch repair: MutS structures bound to mismatches. *Curr Opin Struct Biol* 11, 47-52 (2001)
23. Lamers M. H., A. Perrakis, J. H. Enzlin, H. H. K. Winterwerp, N. Wind & T. Sixma: The crystal structure of DNA mismatch repair protein MutS binding to a G center dot T mismatch. *Nature* 407, 711-717 (2000)
24. Obmolova G., C. Ban, P. Hsieh & W. Yang: Crystal structures of mismatch repair protein MutS and its complex with a substrate DNA. *Nature* 407, 703-710 (2000)

Key Words: SPR, QCM, Biosensors, Thymine-Guanine Mismatch, SNP, MutS, Gene Mutation Detection

Send correspondence to: Dr. Xiaodi Su, Institute of Materials Research and Engineering, 3 Research Link, Singapore 117602. Tel: 65-68748420, Fax: 65-68720785, Email: xd-su@imre.a-star.edu.sg

http://www.bioscience.org/current/vol10.htm